Rational Design and Semisynthesis of Betulinic Acid Analogues as Potent Topoisomerase Inhibitors

Fatma M. Abdel Bar,[†,‡] Mohammad A. Khanfar,[†] Ahmed Y. Elnagar,[†] Hui Liu,[§] Ahmed M. Zaghloul,[‡] Farid A. Badria,[‡] Paul W. Sylvester,[†] Kadria F. Ahmad,[‡] Kevin P. Raisch,[§] and Khalid A. El Sayed*[,†]

Department of Basic Pharmaceutical Sciences, College of Pharmacy, University of Louisiana at Monroe, Monroe, Louisiana 71201, Department of Pharmacognosy, Faculty of Pharmacy, Mansoura University, Mansoura 35516, Egypt, and Department of Radiation Oncology, University of Alabama at Birmingham, Birmingham, Alabama 35294

Received May 20, 2009

Chemical transformation studies were conducted on betulinic acid (**1**), a common plant-derived lupane-type triterpene. Eleven new rationally designed derivatives of **1** (**2**−**5** and **7**−**13**) were synthesized based on docking studies and tested for their topoisomerase I and IIα inhibitory activity. Semisynthetic reactions targeted C-3, C-20, and C-28 in **1**. Structures of the new compounds were confirmed by spectroscopic methods (1D and 2D NMR and MS). Compound **9**, 3-*O*-[*N*-(phenylsulfonyl)carbamoyl-17*β*-*N*-(phenylsulfonyl)amide]betulinic acid, showed 1.5-fold the activity of CPT in a topoisomerase I DNA relaxation assay. Four out of 14 betulinic acid analogues (**5**, **9**, **11**, and **12**) showed 1.5-fold the activity of etoposide in a topoisomerase II assay. The new analogues exhibited better cytotoxic activities against the human colon cancer cells SW948 and HCT-116 and the breast cancer cell line MDA-MB-231 compared to the parent (**1**). Betulinic acid (**1**) is a potential scaffold for the design of new topoisomerase I and IIα inhibitors.

Betulinic, boswellic, ursolic, and oleanolic acids are abundant pentacyclic triterpenes that occur in many edible fruits and vegetables.[1] They have been reported to inhibit topoisomerases I and IIα by competing with DNA for topoisomerase binding through direct interaction via preventing topoisomerase−DNA complex formation.[1] Structure−activity relationship studies suggested that the pentacyclic skeleton and carboxyl group were important pharmacophores for topoisomerase inhibitory activity.[1]

Betulinic acid (**1**) is a common lupane-type pentacyclic triterpene known to exhibit immunomodulation,[2] inhibitory effects on Epstein−Barr virus early antigen activation,[3] and anti-HIV, analgesic, anti-inflammatory, antibacterial, antimalarial, antihelmintic, and antitumor activities.[4] The mechanism of action of **1** has been suggested to be a multitarget inducer of apoptosis.[5,6] It suppressed NF-*κ*B activation through the inhibition of I*κ*Bα kinase and p65 phosphorylation induced by carcinogen and inflammatory stimuli.[5] Thus, **1** inhibited the production of NF-*κ*B-regulated gene products such as cyclooxygenase-2 and matrix metalloproteinase-9.[5−10]

Topoisomerases are essential enzymes that relax DNA supercoiling inside cells during processes such as replication, recombination, and transcription.[11,12] They alter DNA topology by generating transient breaks in the double helix.[11,12] Eukaryotic type I topoisomerases are monomeric enzymes that alter topology by creating transient single-stranded breaks in the DNA. Topoisomerase I functions through three major steps: (a) nucleophilic attack of DNA by the OH group of the active site of topoisomerase I (tyrosine 723, Ty 723), resulting in a covalent attachment of topoisomerase I to the broken DNA strand and formation of a transient phosphotyrosine ester bond between the Tyr 723 and the DNA scissile strand backbone phosphate; (b) DNA unwinding (strand passage or free rotation); and (c) a second transesterification reaction resulting in religation of the DNA strand and dissociation of the topoisomerase I−DNA complex.[14,15]

Eukaryotic type II topoisomerases function as homodimers. The enzyme unwinds, unknots, and untangles the genetic material by generating transient double-stranded breaks in DNA.[13,14] Since type II enzymes cut both strands of the double helix, each protomer subunit contains tyrosine 805, Tyr 805 in the case of human topoisomerase IIα.[13,14] Topoisomerase II initiates DNA cleavage by nucleophilic attack of the active site tyrosine on the phosphate of the nucleic acid backbone.[13] The active site's tyrosine residue of each topoisomerase II protomer subunit becomes covalently linked to the newly generated 5′-terminal phosphate moiety on each strand.[13] This step is followed by strand passage and DNA ligation.[13]

Under normal conditions, topoisomerase−DNA covalent complexes are transient and found at very low levels.[13−15] Stabilization of these complexes generates DNA lesions, inducing cell arrest and apoptosis.[13−15] Compounds that inhibit the catalytic activity of topoisomerase II can be either catalytic inhibitors, which decrease the overall activity of the enzyme, or topoisomerase II poisons, which increase the levels of topoisomerase II−DNA cleavage complex.[13]

In this study, a series of new betulinic acid analogues (**2**−**5** and **7**−**13**) were designed, synthesized, and tested for their ability to inhibit both types of topoisomerases.

Results and Discussion

Molecular Modeling and Docking. To design more active analogues of **1** as topoisomerase inhibitors, a computer-aided molecular modeling study was carried out within the active site of the human topoisomerases I and IIα, starting with the crystal structure of the enzyme bound to DNA (PDB 1t8i and 1bgw for topoisomerases I and IIα, respectively).[16,17] Several analogues of **1** with modified C-3, C-28, and C-20 were proposed and docked to topoisomerase I and IIα active sites. The structures of the topoisomerase I and II inhibitors camptothecin (CPT) and etoposide, respectively, were used as reference molecules in docking and modeling studies.

The active site of topoisomerase I is an arginine- and lysine-rich pocket with condensed positive charge that allows electrostatic interactions with the negatively charged DNA-phosphate backbone. The C-28 COOH group of **1** represents the exclusive binding pharmacophore, generating hydrogen-bonding interactions with the structural skeleton that fit the catalytic residues Arg 488, Lys 532, and Tyr 723, but it is too short to bridge to the other side of the topoisomerase I−DNA binding pocket (Figure 1A). During topoisomerase I-catalyzed DNA supercoiling, Tyr 723 is involved in

* To whom correspondence should be addressed. Tel.: 318-342-1725. Fax: 318-342-1737. E-mail: elsayed@ulm.edu.
[†] University of Louisiana at Monroe.
[‡] Mansoura University.
[§] University of Alabama at Birmingham.

10.1021/np900312u CCC: $40.75
Published on Web 08/19/2009

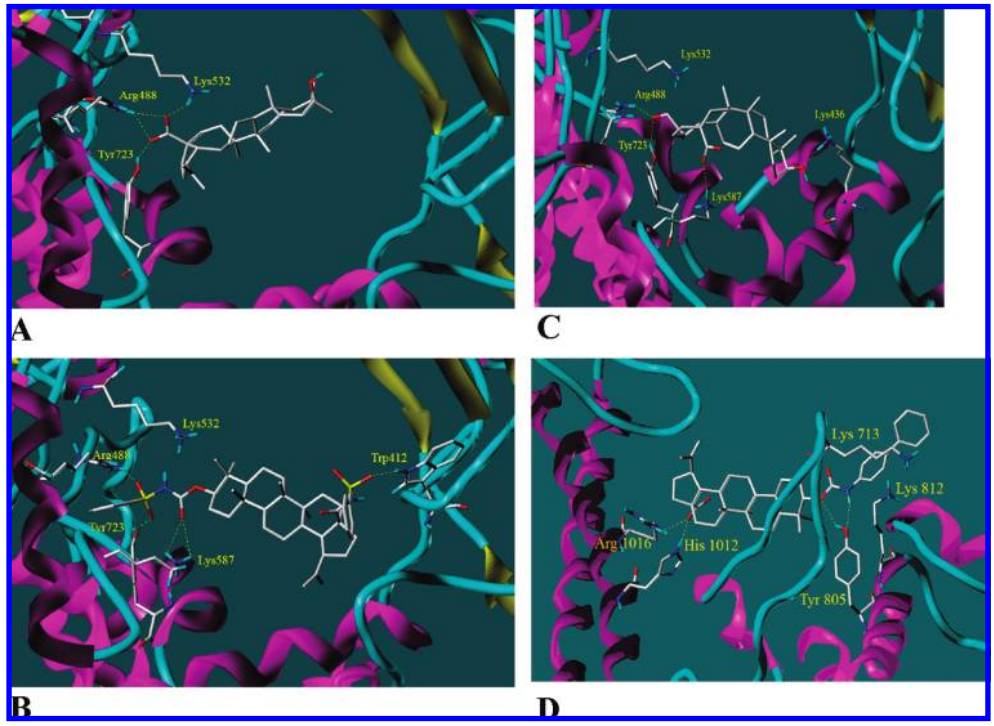

Figure 1. Detailed view of docked structures **1** (A), **9** (B), and **14** (C) with the corresponding interacting amino acids of topoisomerase I, and **11** (D) with topoisomerase IIα binding site.

reversible formation of a 3′-*O*-phospho−tyrosine bond between the active tyrosine site and the cleaved DNA backbone, and therefore this particular amino acid is critical for the enzyme's activity.[18,19]

The aromatic-sulfonyl substitutions at the C-3 OH and C-28 COOH moieties of **1** allow charge-transfer interaction of the π-aromatic cloud with the guanidine and amine groups of arginine and lysine residues, respectively (Table 3). The most active analogue of **1** in the topoisomerase I−DNA relaxation assay (**9**) showed, in addition to interaction of the C-3 side chain π-aromatic cloud mentioned above, the insertion of the C-3 benzenesulfonyl carbamoyl moiety in the positively charged pocket via the H-bonding interactions of the C-1′ carbamate carbonyl with Arg 488 and the interaction of the sulfone group with Lys 587 and the critical conserved catalytic residue Tyr 732 (Figure 1B). Furthermore, the C-28 *N*-phenylsulfonylamide moiety in **9** allows bridging between both sides of the topoisomerase I active site through a complex H-bonding interaction of its sulfone group with Trp 412. These electrostatic interactions were also generated in other aromatic-substituted active analogues, **8** and **13**. Therefore, the topoisomerase I inhibitory activity of **8**, **9**, and **13** can be explained by the blocking of this important catalytic residue, which drastically compromises topoisomerase I activity.

Oxidation of the isopropenyl side chain to C-30 aldehyde in **14** enhanced the topoisomerase I binding affinity (Figure 1C). The C-30 aldehyde group creates H-bond interactions with Arg 488 and Tyr 723 (Figure 1C). The C-28 COOH group binds the Lys 587 residue at one side, while the C-3 OH group binds Lys 436 at the other side (Figure 1C).

Molecular modeling simulations were also applied to understand the interactions of analogues of **1** with topoisomerase IIα. Starting with the crystallographic structure of human topoisomerase IIα available in the RCSB PDB database (code, 1zxm),[20] various possible pockets were identified. ATP, nucleotide, and DNA binding sites were investigated and docked by analogues of **1**. Unfortunately, all docking attempts were unsuccessful, and severe crash or inappropriate superficial bindings were observed. The binding site of the eukaryotic yeast *Saccharomyces cerevisiae* topoisomerase II was previously identified.[21] Human and *S. cerevisiae* DNA topoisomerase II sequences exhibit 47.3% identity and 68.2% similarity.[21] This good sequence similarity, particularly at the DNA-binding domain, allowed molecular modeling simulations and docking studies at the former domain.[21] The conserved amino acids at the DNA-binding domain, Asp 799, Arg 804, and the catalytic residue Tyr 805, were used to direct the protomol generation, and then the search grid was expanded to 15 Å to fit the binding of bulky betulinic acid derivatives.

Similar to topoisomerase I, the *S. cerevisiae* topoisomerase II DNA-binding domain is an arginine- and lysine-rich pocket with condensed positive charge that permits a strong charge-transfer interaction of the π-aromatic cloud of the active betulinic acid analogues (**5**, **8**, **9**, **10**, **11**, and **13**) with guanidine and amine groups of arginine and lysine residues, respectively. Compound **11** showed a strong H-bonding interaction with the catalytic residue Tyr 805, which is a critical amino acid for the enzyme's activity, through the carbamoyl moiety (Figure 1D). The C-28 carboxyl group bridged **11** across the DNA-binding domain and H-bonded to His 1012 and Arg 1016 (Figure 1D). The biphenyl ring in **11** was sandwiched between two positively charged Lys residues, Lys 713 and Lys 812, creating strong electrostatic interactions. Docked poses of compounds **5** and **12** are available in the Supporting Information (Figures S26 and S27, respectively).

Thus, aromatic or olefinic substitutions at C-3 markedly increase the binding affinity of **1** to both topoisomerse types, as indicated by the relatively high docking scores of compounds **5** and **8**−**13** (Table 3). However, oxidation of the isopropenyl side chain to an aldehyde, as in **3** and **14**, enhanced the topoisomerase I docking score without marked effects on topoisomerase IIα binding affinity (Table 3). The C-30 aldehyde group in **14** created H-bond interactions in the case of topoisomerase I with Arg 488 and Tyr 723 (Figure 1C). Thus, compounds **2**−**14** were synthesized and tested for their in vitro topoisomerase I and IIα inhibitory activities.

Semisynthesis of Betulinic Analogues 2−14. Reaction of *m*-chloroperbenzoic acid with **1** afforded products **2** and **3**. The HREIMS, ^{1}H NMR, and ^{13}C NMR data of **2** (Supporting Information, Tables S1 and S2, respectively) indicated epoxidation of the $\Delta^{20,29}$ exomethylene of **1**. The ^{1}H NMR spectrum of **2** showed two

Table 1. ^{1}H NMR Data of Compounds **5**, **9**, **11**, and **12**[a]

	δ_H			
position	**5**	**9**	**11**	**12**
1	1.73, m	0.80, m, 1.54, m	1.02, m, 1.71, m	0.95, m, 1.67, m
2	2.01, m	1.39, m	1.61, m 1.78, m	1.39, m, 1.63, m
3	3.82, m	4.29, dd (10.6, 5.5)	4.50, brd (8.1)	4.33, dd (11.3, 4.0)
5	0.85, m	0.60, m	0.83, m	0.73, m
6	1.24, m, 1.57, m	1.23, m 1.42, m	1.40, m 1.53, m	1.27, m, 1.50, m
7	1.34, m	1.22, m	1.38, m	1.36, m 1.39, m
9	1.24, m	1.04, m	1.25, m	1.22, m
11	1.18, m, 1.45, m	1.11, m	1.28, m 1.43, m	0.88, m, 1.25, m
12	1.64, m	0.85, m 1.49, m	1.15, m 1.70, m	0.98, m 1.64, m
13	2.16, m	2.13, ddd (12.5, 12.5, 3.3)	2.17, ddd (12.4, 12.4, 3.3)	2.13, ddd (12.4, 12.4, 3.3)
15	1.23, m 1.54, m	1.01, m	1.18, m 1.55, m	1.15, m 1.57, m
16	2.13, m, 1.57, m	1.47, m 1.92, dt (14.3, 3.0)	1.42, m 2.28, dt (12.8, 3.0)	1.41, m 2.23, dt (12.8, 3.0)
18	1.41, m	1.45, m	1.61, m	1.55, m
19	2.82, m	2.82, ddd (11.0, 11.0, 4.4)	3.00, ddd (10.3, 10.3, 4.4)	2.96, ddd (11.0, 11.0, 5.1)
21	1.86, m, 1.35, m	1.26, m, 1.61, m	1.40, m, 1.98, m	1.47, m, 1.96, m
22	1.45, m, 2.02, m	1.37, m, 1.75, m	1.44, m, 1.96, m	1.45, m, 1.92, m
23	0.93, s	0.70, 3H, s	0.95, 3H, s	0.87, 3H, s
24	0.75, s	0.73, 3H, s	0.88,3H, s	0.78,3H, s
25	0.79, s	0.72, 3H, s	0.87, 3H, s	0.82, 3H, s
26	0.91, s	0.47, 3H, s	0.95, 3H, s	0.91, 3H, s
27	0.93, s	0.82, 3H, s	0.99, 3H, s	0.96, 3H, s
29	4.58, brs, 4.70, brs	4.52, brs, 4.62, brs	4.63, brs, 4.76, brs	4.59, brs, 4.72, brs
30	1.65, s	1.57, 3H, s	1.71, 3H, s	1.68, 3H, s
2′	7.96, d (8.8)			3.79, brs
3′	6.87, d (8.8)	7.99, d (7.3)[b]	7.48, brs	5.79, ddd (16.8, 10.2, 5.1)
4′		7.51, dd (7.3, 1.5)[c]	7.54, d (8.8)	5.09, dd (10.3, 1.1) 5.15, dd (16.8, 1.5)
5′	6.87, d (8.8)	7.61, dd (8.5, 1.5)[d]		
6′	7.99, d (8.8)	7.51, dd (7.3, 1.5)[c]	7.54, d (8.8)	
7′	3.85, s	7.99, d (7.3)[b]	7.48, brs	
2″		8.03, d (7.3)[b]	7.56, d (8.0)	
3″		7.53, dd (7.3, 1.5)[c]	7.41, dd (8.1, 7.3)	
4″		7.63, dd (8.4, 1.5)[d]	7.30, dd (7.3, 7.3)	
5″		7.53, dd (7.3, 1.5)[c]	7.41, dd (8.1, 7.3)	
6″		8.03, d (7.3)[b]	7.56, d (8.8)	
NH		8.11, brs	6.81, brs	4.69, brs
NH		8.87, brs		

[a] In $CDCl_3$, at 400 MHz. [b−d] Interchangeable in the same column.

oxygenated protons at δ 2.55 (H_2-29), which correlated in HETCOR with the methylene carbon at δ 57.0 (C-29). Protons H_2-29 showed ^2J-HMBC correlations with the quaternary oxygenated carbon at δ_C 60.8 (C-20) and ^3J-HMBC correlations with the C-30 methyl at δ_C 18.0 and the C-19 methine carbon at δ_C 45.5. The *R* configuration at C-20 was indicated by comparing its optical rotation sign ($[\alpha]_D^{25}$ −10.0) with those of the related 3β,28-acetoxy-29-lupanal epimers (20*R*, $[\alpha]_D^{25}$ −103; 20*S*, $[\alpha]_D^{25}$ +70).[22] Thus, **2** was determined to be 20(*R*)-20(29)-epoxybetulinic acid.

The HREIMS and data of **3** suggested a C-29-isopropanal functionality. The NMR data of **3** (Tables S1 and S2) indicated the replacement of the exomethylene H_2-29 protons of **1** with an aldehyde proton doublet (δ_H 9.81 and δ_C 207.0). The COSY spectrum of **3** showed coupling of H-29 with H-20 (δ_H 2.54), which in turn was coupled to the methyl doublet H_3-30 (δ_H 1.10) and H-19 (δ_H 2.40), confirming a 19-isopropanal side chain. The C-20*R* configuration of C-20 was indicated on the basis of the negative sign of optical rotation.[22] Comparison of the ^{13}C NMR data of **3** with messagenic acid C (20*S*-3β-hydroxy-29-oxolupan-28-oic acid) supported the fact that the compounds are C-20 epimers.[23] Therefore, **3** was determined to be 20*R*-3β-hydroxy-29-oxolupan-28-oic acid.

Reaction of **1** with Lawesson's reagent afforded compounds **4** and **5**, while the same reaction with betulonic acid (**6**) afforded **7**. The HREIMS of **4** showed a molecular ion consistent with the molecular formula $C_{30}H_{48}O_2S$, and a pattern of ions with intensity ratios of 95:0.75:4.2, corresponding to the three abundant isotopes of a single sulfur atom. The ^{1}H and ^{13}C NMR data of **4** (Tables S1 and S2) were similar to those of **1**, except that downfield shifts of C-28 and C-17 (+20.0 and +7.9 ppm, respectively) compared to those of **1** indicated replacement of the C-28 carboxylic with a carbothioic group. This was confirmed via observing the ^3J-HMBC correlations of the proton multiplets at δ 1.59 and 2.16 (H-16a and H-16b, respectively) and the proton signals at δ 1.43 and 1.99 (H-22a and H-22b, respectively) with the quaternary thiocarbonyl C-28 (δ_C 203.2). Protons H_2-16 and H_2-22 also showed ^2J-HMBC correlations with the quaternary C-17 (δ_C 64.9). Thus, the structure of **4** was determined to be 28-thiobetulinic acid.

The ^{1}H and ^{13}C NMR data of **5** (Tables 1 and 2) suggested a coupling product with Lawesson's reagent. The HREIMS data of **5** suggested the molecular formula $C_{37}H_{55}O_3PS_3$, indicating a thiobetulinic acid-4-methoxyphenyl phosphonate ester. The ^{13}C NMR data (Table 2) showed a downfield shift of C-3 (δ_C 86.5) versus that of **1** (+9.2 ppm), indicating esterification of this position. This was further supported by the ^3J-HMBC correlation of the methyl singlets H_3-23 and H_3-24 (δ_H 0.93 and 0.75, respectively) with C-3. The ^{1}H NMR spectrum (Table 1) showed an OCH_3 signal at δ 3.85, which showed ^3J-HMBC correlation with the aromatic quaternary carbon C-4′ (δ_C 162.7), confirming the presence of a 4-methoxyphenyl moiety. Aromatic doublets, due to H-2′ and H-6′ (δ_H 7.96 and δ 7.99), showed ^3J-HMBC correlations with C-4′ and COSY couplings with the signal at δ 6.87 (H-3′/5′). H-3′/H-5′ showed a ^3J-HMBC correlation with C-1′ (δ 136.5). The thiocarbonyl signals appeared at δ 203.2 (C-28) and 64.9 (C-17) in a similar pattern to **4**. Thus, the structure of **5** was as indicated.

Oxidation of **1** using with CrO_3 afforded the known betulonic acid (**6**). Reaction of **6** with Lawesson's reagent afforded compound **7**, $C_{30}H_{46}O_2S$, by HREIMS. The ^{1}H and ^{13}C NMR spectra of **7** (Tables S1 and S2) showed a close similarity to those of **6**, except for the downfield shifted quaternary carbons, C-28 (+20.4) and C-17 (+8.4), which indicated the replacement of the carboxylic group with a carbothioic-*O*-acid group. The chemical shift of C-3

Table 2. ^{13}C NMR Data of Compounds **5**, **9, 11**, and **12**[a]

	δ_C			
position	**5**	**9**	**11**	**12**
1	38.6, CH_2	38.3, CH_2	38.5, CH_2	38.1, CH_2
2	26.0, CH_2	23.5, CH_2	24.2, CH_2	24.2, CH_2
3	86.5, CH	85.1, CH	82.5, CH	81.4, CH
4	39.0, qC	38.0, qC	38.1, qC	38.4, qC
5	55.4, CH	55.4, CH	55.6, CH	55.5, CH
6	18.5, CH_2	18.1, CH_2	18.3, CH_2	18.2, CH_2
7	34.3, CH_2	34.2, CH_2	34.3, CH_2	34.3, CH_2
8	40.8, qC	40.6, qC	40.8, qC	40.7, qC
9	50.5, CH	50.5, CH	50.5, CH	50.4, CH
10	37.1, qC	37.0, qC	37.2, qC	37.2, qC
11	20.9, CH_2	20.9, CH_2	21.0, CH_2	20.9, CH_2
12	25.5, CH_2	25.4, CH_2	25.5, CH_2	25.5, CH_2
13	37.5, CH	37.2, CH	38.5, CH	38.5, CH
14	42.5, qC	42.4, qC	42.5, qC	42.5, qC
15	29.5, CH_2	29.3, CH_2	29.8, CH_2	29.8, CH_2
16	33.5, CH_2	32.6, CH_2	32.3, CH_2	32.2, CH_2
17	64.9, qC	57.1, qC	56.5, qC	56.5, qC
18	49.7, CH	49.8, CH	49.3, CH	49.3, CH
19	46.4, CH	45.9, CH	47.1, CH	47.0, CH
20	150.2, qC	150.1, qC	150.5, qC	150.5, qC
21	30.3, CH_2	30.3, CH_2	30.7, CH_2	30.6, CH_2
22	37.8, CH_2	36.7, CH_2	37.2, CH_2	37.2, CH_2
23	28.8, CH_3	27.8, CH_3	28.1, CH_3	28.0, CH_3
24	16.3, CH_3	16.4, CH_3	16.2, CH_3	16.1, CH_3
25	16.8, CH_3	16.2, CH_3	16.3, CH_3	16.3, CH_3
26	16.1, CH_3	15.7, CH_3	16.8, CH_3	16.6, CH_3
27	14.6, CH_3	14.5, CH_3	14.8, CH_3	14.8, CH_3
28	203.2, qC	174.0, qC	182.9, qC	182.0, qC
29	109.9, CH_2	109.8, CH_2	109.9, CH_2	109.8, CH_2
30	19.4, CH_3	19.4, CH_3	19.5, CH_3	19.4, CH_3
1′	136.5, qC	150.6, qC	155.3, qC	156.8, qC
2′	131.9, CH	138.9,[b] qC	137.5, qC	43.5, CH_2
3′	113.8, CH	128.1,[c] CH	119.0, CH	134.8, CH
4′	162.7, qC	129.0, CH	127.7, CH	116.0, CH_2
5′	114.0, CH	133.9,[d] CH	136.2, qC	
6′	132.0, CH	129.0, CH	127.7, CH	
7′		128.1,[c] CH	119.0, CH	
1″		138.8,[b] qC	140.6, qC	
2″		128.3,[c] CH	126.9, CH	
3″		129.0, CH	128.9, CH	
4″		133.8,[d] CH	127.1, CH	
5″		129.0, CH	128.9, CH	
6″		128.3,[c] CH	126.9, CH	

[a] In $CDCl_3$, at 100 MHz. Carbon multiplicities were determined by APT experiment. qC = quaternary, CH = methine, CH_2 = methylene, CH_3 = methyl carbons. [b−d] Interchangeable in the same column.

(δ_C 218.4) was similar to that of **6**. The methyl singlets due to H_3-23 and H_3-24 showed ^3J-HMBC correlations with C-3. This confirmed the ketone at C-3 and the structure of **7** to be 28-thiobetulonic acid.

Carbamoylation of **1** by reaction with different isocyanates afforded compounds **8**−**12**. The HREIMS data of **8** showed a molecular ion peak at *m/z* 589.4139 ($C_{38}H_{55}NO_4$ and 12 degrees of unsaturation). Downfield shifts of the H-3 and C-3 signals in **8** (+1.22 and +4.2 ppm, respectively) compared to those of **1** suggested possible carbamoylation at C-3. The ^1H and ^{13}C NMR data supported this and were comparable to those of **1** with additional C-3-*O*-[*N*-(benzyl)carbamoyl] moiety signals. The carbonyl carbon at δ_C 156.9 was assigned C-1′ on the basis of its ^2J-HMBC correlation with the H_2-2′ multiplet (δ_H 4.32). The H_2-2′ protons also showed ^2J-HMBC correlations with C-3′ (δ_C 138.7) and ^3J-HMBC correlations with the methine carbons C-4′ and C-8′ (δ_C 127.6). The proton doublet H_2-4′/8′ (δ_H 7.27) showed a ^3J-HMBC correlation with the methine carbon C-6′ (δ_H 127.5), while the H_2-5′/7′ (δ_H 7.31) signal showed a ^3J-HMBC correlation with the quaternary carbon C-3′, confirming the 3-*O*-[*N*-(benzyl)carbamoyl] side chain. Thus, the structure of **8** was proved to be as indicated.

The ^1H NMR spectrum of **9** (Table 1) showed 10 aromatic protons, indicating two phenyl substitutions. The downfield shifts of H-3 and C-3 signals in **9** versus those of **1** suggested carbamoylation at C-3 (Tables 1 and 2). The ^{13}C NMR data (Table 2) showed an upfield shift of C-28 (−9.7 ppm) compared to that of **1**, suggesting a change at this position. The reaction of COOH groups with sulfonyl isocyanates to produce *N*-acylsulfonylamides has been documented.[24] A broad singlet at δ_H 8.87 was assigned to the NH proton of an *N*-phenylsulfonylamide moiety at C-28 (δ_C 174.0). This was based on its ^2J-HMBC correlation with the C-28 amide carbonyl. The HREIMS data ($C_{43}H_{58}N_2O_7S_2$) were consistent with phenylsulfonylcarbamoyl and *N*-phenylsulfonylamide moieties. NMR assignments were based on HETCOR and HMBC data. Protons H-4′/6′ (δ_H 7.51) showed ^3J-HMBC correlation with the quaternary carbon at δ 138.9 (C-2′), while H-3′/7′ (δ_H 7.99) showed ^3J-HMBC correlation with the aromatic methine carbon at δ 133.9 (C-5′). Protons H-3″/5″ (δ_H 7.53) showed ^3J-HMBC correlation with the quaternary carbon at δ 138.8 (C-1"), while H-2″/6″ (δ_H 8.03) showed a similar correlation with the methine carbon at δ 133.8 (C-4″). Thus, the structure of **9** was determined to be as shown.

Compound **10** had the molecular formula $C_{41}H_{55}NO_4$, indicating the presence of a naphthyl carbamoyl moiety. The ^1H NMR data of **10** showed a downfield shift of H-3 (+1.3 ppm), suggesting carbamoylation at C-3. The ^{13}C NMR spectrum revealed line broadening of five carbon signals at 21 °C. In the HMQC spectrum, C-3 showed a cross-peak with H-3 (δ_H 4.50) and a broad carbon signal at δ 83.0. The methyl singlets H_3-23 and H_3-24 supported this assignment via their ^3J-HMBC correlations to C-3. Similarly, the proton signals at δ 7.64 and 7.90 showed cross-peaks in HMQC with broad carbon signals at δ 123.3 and 119.0 (C-5′ and C-6′). H-4′ and H-5′ confirmed this assignment through their HMBC correlations with C-5′ and C-6′, respectively. The HMBC spectrum revealed a fourth very broad quaternary carbon signal at δ 136.0 (C-2′), which was correlated with both H-4′ and H-9′. The line broadening of these carbons may be attributed to the steric effect of the bulky naphthyl carbamoyl moiety.[25] Thus, the structure of **10** was determined to be as shown.

Analysis of HREIMS of **11** ($C_{43}H_{57}NO_4$) indicated the presence of a biphenyl carbamoyl moiety. The ^1H NMR data of **11** (Table 1) showed nine aromatic protons and a downfield shifted H-3, confirming biphenyl carbamoylation at C-3. Due to the steric effect of the bulky biphenyl carbamoyl group,[25] the ^{13}C NMR spectrum of **11** revealed line broadening of carbon signals for C-3, C-1′, and C-3′/7′. Assignments of these carbons were based on extensive analysis of HETCOR and HMBC data. The biphenyl system was confirmed via the ^3J-HMBC correlations of the proton doublet H-3′/7′ (δ_H 7.43) with the quaternary carbon signal at δ 140.6 (C-1″) and the proton doublet H-2″/6″ (δ_H 7.56) with the quaternary carbon C-2′ (δ_C 137.5). Thus, the structure of **11** was determined to be the 3-*O*-[*N*-(biphenyl)-*p*-carbamoyl] derivative of betulinic acid.

Compound **12** had the molecular formula $C_{34}H_{53}NO_4$, and ^{13}C NMR data (Tables 1 and 2) indicated that it was a C-3-*O*-[(*N*-allyl)-carbamoyl] derivative of **1**. H-3′ (δ_H 5.79) showed COSY couplings with H-4′a (δ_H 5.09) and H-4′b (δ_H 5.15) and the broad singlet H_2-2′ (δ_H 3.79), indicating an allyl side chain. The nitrogenated methylene carbon C-2′ (δ_C 43.5) was assigned on the basis of its ^3J-HMBC correlation with H_2-4′. The olefinic methine carbon C-3′ (δ_C 134.8) showed a ^2J-HMBC correlation with H_2-4′. Thus, the structure of **12** was determined to be as shown.

The HREIMS and NMR data of **13** suggested benzenesulfonation of **1** at C-3. The ^1H NMR spectrum of **13** showed five aromatic protons. The ^{13}C NMR data showed three methine carbons at δ 127.7 (C-2′/6′), 129.1 (C-3′/5′), and 133.4 (C-4′) in addition to a quaternary at δ 137.9 (C-1′), confirming the benzenesulfonyl moiety. The HMBC spectrum showed ^3J-HMBC correlations of the methyl singlets H_3-23 and H_3-24 (δ_H 0.77 and 0.76, respectively)

Table 3. Inhibition of Cell Proliferation, Topoisomerases I and IIα Inhibitory Activity, and Virtual Binding Affinity of Betulinic Acid (**1**) and Analogues **2**−**14**

compound	IC_{50} [μM][a] SW948	HCT-116	MDA-MB-231	topoisomerase I inhibition [100 μM][b]	topoisomerase I total docking score[c]	topoisomerase IIα inhibition [100 μM][b]	topoisomerase IIα total docking score[c]
1	10.50 ± 3.07	13.46 ± 0.22	15.24	1+	4.03	0	2.66
2	>25	>25	4.08	1+	3.90	0	2.91
3	>25	>25	0.17	2+	4.27	0	2.99
4	>25	>25	>25	1+	3.30	2+	3.05
5	>25	>25	9.83	2+	4.40	3+	5.31
6	19.17 ± 0.37	2.61 ± 0.41	9.77	0	3.23	0	2.94
7	>25	>25	>25	1+	3.30	1+	3.03
8	>25	22.24 ± 2.40	0.45	2+	4.46	2+	5.63
9	17.37 ± 0.24	13.34 ± 3.00	0.92	3+	5.09	3+	3.80
10	>25	>25	>25	1+	4.05	2+	5.65
11	>25	>25	>25	1+	4.65	3+	4.90
12	17.62 ± 1.30	17.73 ± 2.06	0.65	1+	4.50	3+	5.28
13	6.84 ± 1.04	21.26 ± 1.65	0.80	1+	5.18	2+	4.75
14	14.88 ± 0.84	4.38 ± 0.04	1.37	2+	5.07	0	2.78
CPT	0.16 ± 0.06	0.13 ± 0.03	ND	2+	4.89	ND	ND
Etoposide	1.3 ± 0.2	1.7 ± 0.2	ND	ND	ND	2+	4.62

[a] Concentration of betulinic acid analogues that inhibit 50% cell proliferation (IC_{50}). [b] Topoisomerase inhibitory activity was scored as 3+ (strong), 2+ (moderate), 1+ (weak), and 0 (none), with the positive control drug CPT (topoisomerase I assay) or etoposide (topoisomerase II assay) scoring 2+. [c] Virtual binding affinity of compounds **1**−**14** for human topoisomerase I (PDB code: 1t8i) or topoisomerase IIα (PDB code: 1bgw) using SYBYL 8.1 Surflex-Docking, the total score was expressed in $-\log(K_d)$ units to represent binding affinities.

with the downfield methine carbon signals at δ 91.5 (C-3), confirming benzenesulfonation at C-3.

Oxidation of **1** with SeO_2 afforded compound **14**, which proved to be the known messagenic acid F.[15] It is worth noting that the presence of the C-30 aldehyde group restricted rotation of the C-20 side chain, which causes severe line broadening of several nearby carbons (C-18, C-19, C-20, C-21, and C-29), resulting in their disappearance into noise.[25] This led to the incorrect assignment of some of these carbon signals in the published NMR data.[23] The HMBC spectrum of **14** showed ^3J-HMBC correlation of the proton signals at δ 5.88 (H-29b) and 6.26 (H-29b) with the methine carbons C-30 (δ_C 195.4) and C-19 (δ_C 38.2), leading to the unambiguous assignment of these carbons. The ^2J-HMBC correlation of the aldehyde proton singlet H-30 (δ_H 9.46) with the broad carbon signal at δ 157.2 confirmed the assignment as C-20. H-22b (δ_H 1.89), H-21a (δ_H 1.92), and H-16b (δ_H 2.23) showed ^3J-HMBC correlations with the broad carbon signal at δ 53.1, leading to the assignment of this carbon as C-18. Finally, the ^2J-HMBC correlation of H-22b with the broad signal at δ 25.0 suggested the assignment of this as C-21.

Topoisomerase I−DNA Relaxation Assay.[26] Inhibition of topoisomerase function constitutes a useful strategy for the identification of potential antitumor agents. Betulinic acid derivatives were tested using topoisomerase I−DNA relaxation assay and compared to the known natural topoisomerase I inhibitor CPT. Reaction mixtures were analyzed by agarose gel electrophoresis. Figure 2A and Table 3 show the catalytic inhibition of topoisomerase I by **1** and derivatives **2**−**14** as shown in lanes 5−18 at 100 μM in comparison to 100 μM camptothecin (lane 4). Compounds **3**, **5**, **8**, and **14** (Figure 2aA, lanes 5, 18, 7, and 6, respectively) showed topoisomerase I inhibitory activities comparable to CPT. Compound **9** (lane 9) showed the highest inhibitory activity toward relaxation of supercoiled DNA with activity greater than that of CPT.

Inhibition of Decatenation of kDNA by Topoisomerase II Enzyme.[26] Compounds **1**−**14** were also screened for their ability to inhibit topoisomerase II enzymatic activity, with etoposide as a positive control.[26] Nine of the compounds exhibited inhibition of topoisomerase II catalytic activity (Figure 2bB and Table 3). Of these, four compounds (**5**, **9**, **11**, and **12**) showed 1.5-fold better inhibition of the catalytic activity of topoisomerase II compared to etoposide (Figure 2B, lanes 17, 8, 12, and 14, respectively).

The above results show a rational correlation of topoisomerase I and II inhibitory activities with the virtual binding affinity of the selected analogues (Table 3) and indicated the potential of the readily available natural triterpene betulinic acid (**1**) as a scaffold for the design of additional topoisomerase inhibitors.

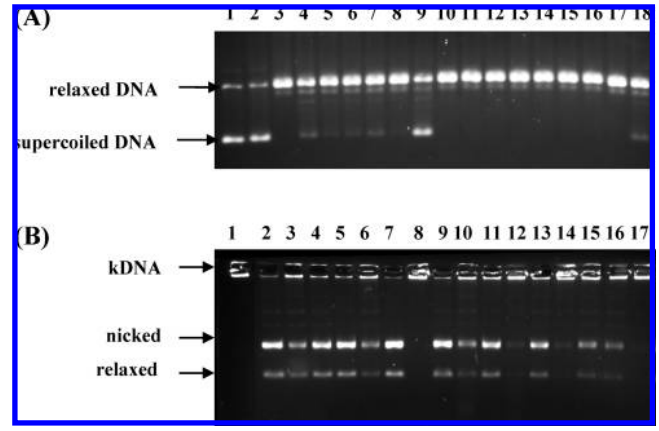

Figure 2. (A) Catalytic inhibition of topoisomerase I by betulinic acid derivatives. Lane 1, supercoiled plasmid DNA alone (250 ng); lane 2, same as lane 1 + 0.5% DMSO; lane 3, same as lane 1 + topoisomerase I (2U); lane 4, topoisomerase I (2U) + 100 μM camptothecin and DNA. Lanes 5−18, topoisomerase I (2U) + DNA and 100 μM betulinic acid analogues: lane 5 (**3**); lane 6 (**14**); lane 7 (**8**); lane 8 (**2**); lane 9 (**9**); lane 10 (**6**); lane 11 (**10**); lane 12 (**1**); lane 13 (**11**); lane 14 (**7**); lane 15 (**12**); lane 16 (**4**); lane 17 (**13**); lane 18 (**5**). (B) Topoisomerase II inhibitory assay by betulinic acid derivatives. Lane 1, kinetoplast DNA (kDNA) alone; lane 2, same as lane 1 + topoisomerase II (2U); lane 3, the same as lane 2 + 100 μM etoposide. Lanes 4−17, topoisomerase II (2U) + kDNA and 100 μM betulinic acid analogues: lane 4 (**3**); lane 5 (**14**); lane 6 (**8**); lane 7 (**2**); lane 8 (**9**); lane 9 (**6**); lane 10 (**10**); lane 11 (**1**); lane 12 (**11**); lane 13 (**7**); lane 14 (**12**); lane 15 (**4**); lane 16 (**13**); lane 17 (**5**).

Inhibition of Cell Proliferation Activity. Although colon cancer cells were reported to be almost completely refractory to treatment with **1** and its derivatives,[27] most of new analogues showed IC_{50} values < 20 μM (Table 3). Analogue **13**, with a benzenesulfonyl moiety at C-3, showed good activity against SW948 colon cancer cells (IC_{50} 6.84 μM). Analogues **6** and **14** showed good activity against HCT-116 colon cancer cells (IC_{50} 2.61 and 4.38 μM, respectively).

Scheme 1. Preparation of Compounds **2** and **3**[a]

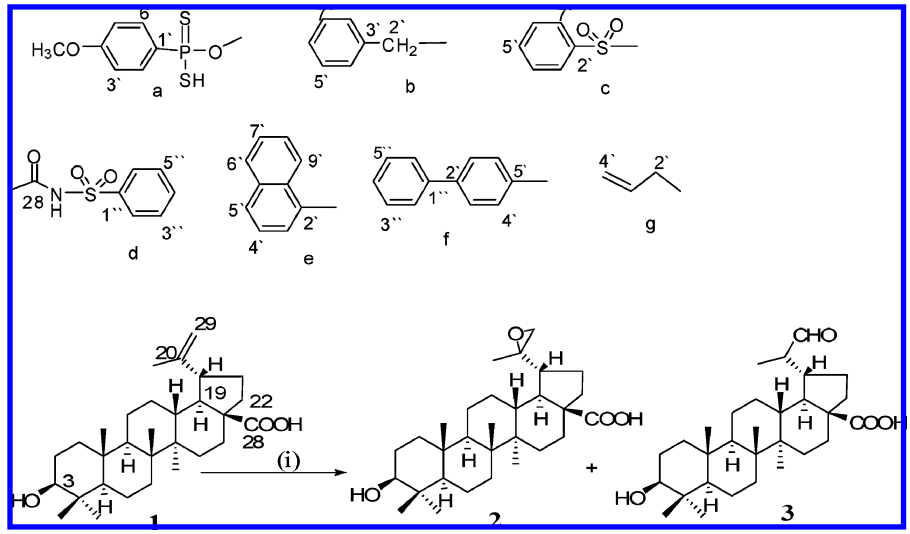

[a] Reagents and conditions: (i) *m*-CPBA, CH_2Cl_2, 1 h, rt.

MDA-MB-231 breast cancer cells showed less resistance to the test compounds than the colon cancer cell lines. Compounds **3**, **8**, **9**, **13**, and **14** showed remarkable activities against MDA-MB-231 cells, with IC_{50}'s of 0.17, 0.45, 0.92, 0.80, and 1.37 μM, respectively, compared to **1** (IC_{50} 15.24 μM). The most potent compound, **3**, is a dihydrobetulinic acid analogue, which has been reported to be more cytotoxic and a better topoisomerase I inhibitor than **1**.[8,9] The marked variations in cytotoxicity results compared to topoisomerase I inhibitory activities of the derivatives may indicate that **1** is a multitarget inducer of apoptosis.

Compound **4**, with a C-28 thiocarboxylic acid group, was tested by the Developmental Therapeutics Program (DTP) against the 60 human cell line panel at a 10 μM dose. These results (Figure S25, NSC749378) showed better cytotoxicity than **1**, indicating that a C-28 thiocarboxy group is better than a carboxy group for cytotoxic activity.

Conclusions. Eleven new rationally designed analogues of **1** were synthesized on the basis of molecular modeling studies and tested for their topoisomerase I and IIα inhibitory activity. Semisynthetic reactions targeted C-3, C-28, and C-20 in **1**. Compounds **3**, **5**, **8**, **9**, and **14** showed topoisomerase I inhibitory activities comparable to or better than CPT. Nine out of 14 compounds inhibited topoisomerase II catalytic activity, of which **5**, **9**, **11**, and **12** showed 1.5-fold better activity than etoposide. Aromatic or olefinic substitutions at C-3 markedly increased the binding affinity toward both topoisomerse types, while oxidation of the isopropenyl side chain to an aldehyde enhanced the topoisomerase I activity without marked effects on topoisomerase IIα binding affinity. The readily available natural product betulinic acid is a potential scaffold for the design of potent topoisomerase inhibitors.

Experimental Section

General Experimental Procedures. Optical rotations were determined on a Rudolph Research Analytical Autopol III polarimeter. IR spectra were recorded on a Varian 800 FT-IR spectrophotometer. ^1H and ^{13}C NMR spectra were recorded in $CDCl_3$, using TMS as an internal standard, on a JEOL Eclipse NMR spectrometer operating at 400 MHz for ^1H and 100 MHz for ^{13}C. HREIMS and HRESMS experiments were conducted at the University of Michigan on a Micromass LCT spectrometer. TLC analyses were carried out on precoated silica gel 60 F_{254} 500 μm TLC plates, using the developing systems *n*-hexane−EtOAc (9:1, 8:2, or 6:4). Silica gel 60 (EMD Chemicals Inc.), 70−230 mesh, or silica gel (Natland International Corporation), 230−400 mesh, was used for column chromatography.

Scheme 2. Preparation of Compounds **4**, **5**, and **7**[a]

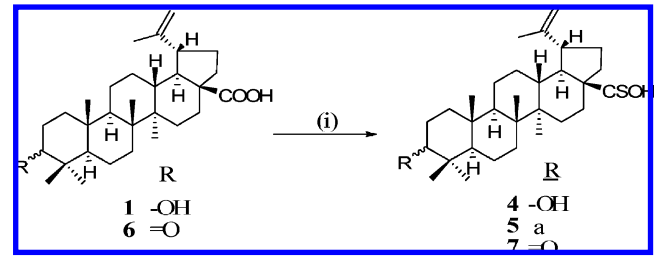

[a] Reagents and conditions: (i) Lawesson's reagent, toluene, 110 °C, 3 h.

Plant Material. Betulinic acid (**1**) was isolated and purified from a methanolic extract of leaves of *Melaleuca ericifolia* grown in Egypt.[4]

Preparation of Compounds 2 and 3.[28] To a solution of **1** (90 mg, 0.2 mmol) in CH_2Cl_2 (2.5 mL) was added 70% *m*-chloroperoxybenzoic acid (*m*-CPBA) (59 mg, 0.24 mmol, Scheme 1). The solution was stirred for 1 h at room temperature, after which 10% aqueous Na_2SO_3 (10 mL) was added. The aqueous solution was extracted twice with $CHCl_3$. The combined organic layers were washed with saturated $NaHCO_3$ and brine and then dried under vacuum. The crude product was chromatographed on silica gel 60 using *n*-hexane−EtOAc (8:2) to give **2** (60 mg, 66%) and **3** (10 mg, 11%).

Preparation of Compounds 4, 5, and 7.[29] Equimolar quantities of **1** (100 mg) or **6** (50 mg) and Lawesson's reagent (88 or 44 mg, respectively) were dissolved in 3 or 1.5 mL of toluene (Scheme 2). Each mixture was stirred and heated at 110 °C for 3 h. The reaction was then quenched by addition of water (10 mL). The mixture was extracted with ethyl acetate (3 × 10 mL). The ethyl acetate extract was evaporated under vacuum, and the crude product was purified over Si gel 60 using an *n*-hexane−EtOAc (9:1), isocratic, to give **4** (48 mg, 48%) and **7** (34 mg, 68%), or *n*-hexane−EtOAc (4:6) to give **5** (17 mg, 17%).

Oxidation of 1 to 6. A solution of betulinic acid (100 mg) in a mixture of toluene (1 mL) and acetonitrile (0.5 mL) was stirred with CrO_3 (100 mg) at room temperature for 1 h (Scheme 1).[30] Water was then added, and the mixture was extracted with $CHCl_3$ (3 × 10 mL). The chloroform extract was dried over anhydrous $NaSO_4$ and evaporated under vacuum. The solid product was purified over Si gel 60 using *n*-hexane−EtOAc (9:1) to give betulonic acid **6** (80 mg, 80%).[30]

Preparation of Carbamates 8−12.[31] To a solution of **1** (100 mg) in toluene (3 mL) was added an equivalent amount of benzyl isocyanate (29.0 mg), allyl isocyanate (18.3 mg), 4-biphenyl isocyanate (42.9 mg), 1-naphthyl isocyanate (37.2 mg), or benzene sulfonyl isocyanate (40.7 mg), and the solutions were separately mixed with 15 μL of Et_3N and refluxed for 1 h (Scheme 3). Water (10 mL) was then added, and each

Scheme 3. Preparation of Compounds **8**−**14**[a]

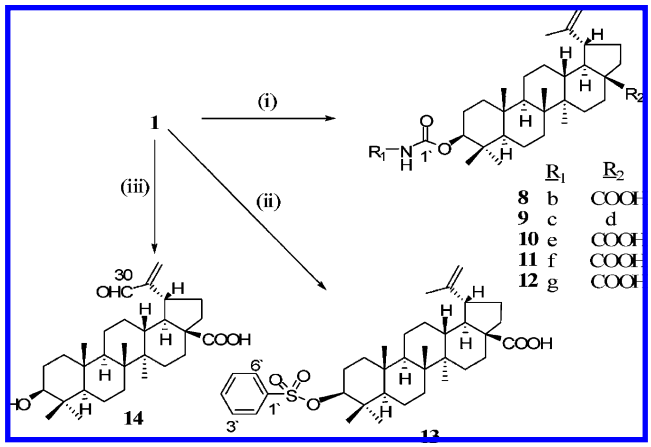

[a] Reagents and conditions: (i) R_1-N=C=O/toluene, Et_3N, reflux, 1 h; (ii) benzenesulfonyl chloride−pyridine, 48 h, rt; (iii) SeO_2/dioxane, 24 h, rt.

reaction product was extracted with EtOAc (3 × 10 mL). The ethyl acetate extract was dried over anhydrous Na_2SO_4 and evaporated under vacuum. The crude products were then purified over Si gel 60 using *n*-hexane−EtOAc (9:1 or 8:2) to give **8** (90 mg, 90%), **9** (98 mg, 98%), **10** (71 mg, 71%), **11** (93.5 mg, 93.5%), and **12** (53 mg, 53%).

Preparation of Compound 13. To a solution of **1** (100 mg) in pyridine (3 mL) was added benzenesulfonyl chloride (40 mg), and the mixture was stirred for 48 h at room temperature (Scheme 3). The reaction was stopped by addition of water and extracted with EtOAc (3 × 10 mL). The combined EtOAc extract was dried over anhydrous Na_2SO_4 and evaporated under vacuum. The crude product was purified over Si gel 60 using *n*-hexane−EtOAc (9.5:0.5) to give **13** (28 mg, 28%).

Preparation of Compound 14. SeO_2 (50 mg) was added to a solution of **1** (100 mg) in anhydrous dioxane (5 mL) (Scheme 3). The reaction mixture was stirred for 24 h at room temperature. Water was then added, and the mixture was extracted with $CHCl_3$ (3 × 10 mL). The combined $CHCl_3$ extract was dried over anhydrous Na_2SO_4 and evaporated under vacuum. The crude product was chromatographed on Si gel 60 using *n*-hexane−EtOAc (8:2) to give **14** (40 mg, 40%).

Cell Lines. Cells were purchased from the American Type Culture Collection (ATCC, Manassas, VA) and propagated as recommended by ATCC. HCT-116 cells were maintained on modified McCoy's 5a medium, and SW948 cells were maintained on Leibovitz's L-15 medium. Both culture media were supplemented with 10% heat-inactivated FBS and 2 mM L-glutamine. The human breast cancer cell line MDA-MB-231 was maintained in RPMI 1640 medium supplemented with 10% heat-inactivated fetal bovine serum and 25 mM HEPES. Cell cultures were maintained at 37 °C in a humidified atmosphere of 5% CO_2 in an incubator.

Inhibition of DNA Relaxation by Topoisomerase I Enzyme. Topoisomerase I drug screening kit (TopoGen, Inc., Port Orange, FL) was used to determine the inhibitory activity of **1**−**14** to block or reduce topoisomerase I DNA relaxation activity. For this assay, 250 ng of supercoiled plasmid DNA was added to the assay buffer (10 mM Tris-HCl, pH 7.9, 1 mM EDTA, 150 mM NaCl, 0.1% BSA, 0.1 mM spermidine, and 5% glycerol), followed by tested compound or camptothecin at a final concentration of 100 μM. Equal concentrations of DMSO (0.5%) were maintained in each reaction mixture so as not to produce solvent-mediated inhibition of topoisomerase I activity. Topoisomerase I (2U) was added to the assay mixture, and reactions were carried out at 37 °C for 30 min, then terminated by addition of 1% SDS (sodium dodecyl sulfate). The reaction mixtures were digested with proteinase K (50 μg/mL) for 30 min at 37 °C followed by chloroform−isoamyl alcohol extraction. The aqueous phase was collected, and DNA was separated by electrophoresis in a 1% agarose gel in TAE buffer (40 mM Tris-acetate, 1 mM EDTA) at 1 V/cm for 16 h at room temperature. The agarose gels were stained with ethidium bromide (0.5 μg/mL) and extensively destained in water, and the DNA bands were visualized by transillumination with UV light (320 nm) and quantified using the Kodak Gel Logic 200 imaging system and molecular imaging software (Eastman Kodak Co., Rochester, NY). The ability of each drug to inhibit topoisomerase I activity was scored as 3+ (strong), 2+ (moderate), 1+ (weak), and 0 (none), with the positive control drug CPT scoring 2+.

Inhibition of Decatenation of kDNA by Topoisomerase II Enzyme. Compounds **1**−**14** were screened for the ability to inhibit the decatenation of kDNA using a Topoisomerase II assay kit (TopoGen, Inc., Port Orange, FL).[26] Briefly, 100 μM of each compound or etoposide was incubated with kinetoplast DNA (kDNA) and 2U topoisomerase II enzyme for 15 min at 37 °C.[26] The reactions were stopped and separated by 1% agarose gel electrophoresis containing ethidium bromide (0.5 μg/mL). After destaining in water, the kDNA, nicked circular DNA, and relaxed circular DNA were detected and quantified using the Kodak Gel Logic 200 imaging system and Molecular Imaging software. The data were then analyzed using Excel (Microsoft, Inc., Redmond, WA). The ability of each tested compound to inhibit topoisomerase II activity was scored as 3+ (strong), 2+ (moderate), 1+ (weak), and 0 (none), with the positive control drug etoposide scoring 2+.

Cell Proliferation Assays. Antiproliferative activities of **1** and analogues on colon cancer cells were assessed using the XTT microtiter plate tetrazolium-based cell proliferation assay (R & D Systems Inc., Minneapolis, MN). For the XTT assay, 4000 cells were plated per well into a 96-well plate. After 1-day growth at 37 °C, various concentrations of the drug were added per well. The plates were incubated for an additional 3 days and then analyzed using a plate reader (Molecular Devices Corp., Sunnyvale, CA) after the addition of XTT reagent as described by the manufacture's protocol. Each drug concentration was done in triplicate, and the results were analyzed using a linear-quadratic equation to determine the concentration of drug that inhibited 50% of the cell proliferation (IC_{50}). The inhibition of cell proliferation assays were repeated two or three times, and the mean ± SE of the IC_{50} for each drug was determined. All compounds were compared to the IC_{50} determinations of camptothecin.

The cytotoxic properties of betulinic acid analogues on MDA-MB-231 were assessed using the MTT cytotoxicity assay described before.[32] Briefly, about 15 000 cells/well were plated into a 96-well plate. Inoculates were allowed a preincubation period of 1 day at 37 °C. All test compound doses were evaluated in triplicate. Incubation of the cells with the test compounds lasted for 3 days at 37 °C. At the end of the incubation period, the cells were assayed using MTT, Trevogen. Aliquots (10 μL) of the MTT stock solution were added to each well and incubated for 4 h. Then, formazan produced was dissolved by the addition of 100 μL/well of detergent reagent, Trevogen, followed by a further incubation at room temperature overnight in the dark. The optical density (OD) was measured at 580 nm using a BioTeck microplate reader against a blank prepared from cell-free cultures. The number of cells/well was calculated using a calibration curve. The IC_{50} values were calculated from appropriate dose−response curves.

Molecular Modeling and Docking. Three-dimensional structure building and all modeling were performed using the SYBYL program package,[33] version 8.1, installed on Dell desktop workstations equipped with a dual 2.0 GHz Intel Xeon processor running the Red Hat Enterprise Linux (version 5) operating system. Conformations of each compound were generated using Confort conformational analysis. Energy minimizations were performed using the Tripos force field with a distance-dependent dielectric and the Powell conjugate gradient algorithm with a convergence criterion of 0.01 kcal/(mol A).[34] Partial atomic charges were calculated using the semiempirical program MOPAC 6.0 and applying the AM1.[35]

Surflex-Dock program version 2.0 interfaced with SYBYL 8.1 was used to dock the betulinic acid analogues to the topoisomerase I and II active sites.[36,37] Surflex-Dock employs an idealized active site ligand (protomol) as a target to generate putative poses of molecules or molecular fragments.[38,39] These poses were scored using the Hammerhead scoring function.[38,39] Surflex-Dock uses an empirically derived scoring function that is based on the binding affinities of protein−ligand complexes based on their X-ray structures. Surflex-Dock provides accurate scoring function that is derived from the known binding affinity data and negative training data to reduce false positive binding scores.[38,39] The scoring function includes the following terms: hydrophobic, polar, repulsive, entropic, and solvation energies. Surflex-Dock scores are expressed in $-\log 10(K_d)$ units to represent the binding affinities.[38,39]

The 3D structures of topoisomerases I and II were taken from the Brookhaven Protein Databank (PDB codes: 1t8i and 1bgw, respectively).[16,17] Topoisomerase I was prepared by removal of DNA double helix and removal of the phosphate group at Tyr 723, followed by minimization.

20(*R*)-20(29)-Epoxybetulinic Acid (2): amorphous solid, $[\alpha]_D^{25}$ −10.0 (*c* 0.43, $CHCl_3$); IR ν_{max} ($CHCl_3$) 3511, 3188, 2946, 2869, 1710, 1461, 1377, 1136, 1107, 983, 901 cm^{-1}; ^1H and ^{13}C NMR, see Tables S1 and S2, Supporting Information; HREIMS *m/z* 472.3570 $[M]^+$ (calcd for $C_{30}H_{48}O_4$, 472.3553).

20*R*-3*β*-Hydroxy-29-oxolupan-28-oic Acid (3): amorphous solid, $[\alpha]_D^{25}$ −25.0 (*c* 0.40, $CHCl_3$); IR ν_{max} ($CHCl_3$) 3510, 3155, 2947, 2869, 1716, 1694, 1456, 1364, 1134, 1029, 865 cm^{-1}; ^1H and ^{13}C NMR, see Tables S1 and S2, Supporting Information; HREIMS *m/z* 472.3541 $[M]^+$ (calcd for $C_{30}H_{48}O_4$, 472.3553).

28-Thiobetulinic Acid (4): amorphous solid, $[\alpha]_D^{25}$ +1.7 (*c* 0.12, $CHCl_3$); IR ν_{max} 3605, 2991, 2947, 2868, 1694, 1642, 1598, 1462, 1378, 1113, 981, 893, 834 cm^{-1}; ^1H and ^{13}C NMR, see Tables S1 and S2, Supporting Information; HREIMS *m/z* 471.3298 $[M - H]^-$ (calcd for $C_{30}H_{47}O_2S$, 471.3297).

3-*O*-*β*-[Mercapto(4-methoxyphenyl)phosphorothioyloxy]betulinic Acid (5): amorphous solid, $[\alpha]_D^{25}$ −90 (*c* 0.14, $CHCl_3$); IR ν_{max} 3405, 3020, 2975, 2947, 2866, 1698, 1597, 1460, 1114, 975, 892, 838 cm^{-1}; ^1H and ^{13}C NMR, see Tables 1 and 2; HREIMS *m/z* 673.2980 $[M - H]^-$ (calcd for $C_{37}H_{54}O_3PS_3$, 673.2973).

28-Thiobetulonic Acid (7): amorphous solid, $[\alpha]_D^{25}$ +29.8 (*c* 0.57, $CHCl_3$); IR ν_{max} 3515, 2989, 2946, 2867, 1696, 1647, 1460, 1378, 1115, 969, 949, 894 cm^{-1}; ^1H and ^{13}C NMR, see Tables S1 and S2, Supporting Information; HREIMS *m/z* 469.3162 $[M - H]^-$ (calcd for $C_{30}H_{45}O_2S$, 469.3140).

3-*O*-[*N*-(Benzyl)carbamoyl]betulinic Acid (8): amorphous solid, $[\alpha]_D^{25}$ +17.4 (*c* 3.2, $CHCl_3$); IR ν_{max} ($CHCl_3$) 3450, 3316, 3161, 2989, 2946, 2870, 1712, 1698, 1642, 1496, 1456, 1376, 1135, 1106, 976, 891 cm^{-1}; ^1H and ^{13}C NMR, see Table S3, Supporting Information; HREIMS *m/z* 589.4139 $[M]^+$ (calcd for $C_{38}H_{55}NO_4$, 589.4131).

3-*O*-[*N*-(Phenylsulfonyl)carbamoyl-17*β*-*N*-(phenylsulfonyl)amide]-betulinic Acid (9): amorphous solid, $[\alpha]_D^{25}$ +8.4 (*c* 1.76, $CHCl_3$); IR ν_{max} 3390, 3264, 3076, 2949, 2872, 1744, 1723, 1451, 1402, 1351, 1294, 1162, 1090, 963, 887, 841, 604, 574 cm^{-1}; ^1H and ^{13}C NMR, see Tables 1 and 2; HREIMS *m/z* 777.3604 $[M - H]^-$ (calcd for $C_{43}H_{57}N_2O_7S_2$, 777.3607).

3-*O*-[*N*-(1-Naphthyl)carbamoyl]betulinic Acid (10): amorphous solid, $[\alpha]_D^{25}$ +14.4 (*c* 0.24, $CHCl_3$); IR ν_{max}, 3432, 3178, 2989, 2949, 2873, 1724, 1699, 1493, 1363, 1105, 1005, 974, 891, 600 cm^{-1}; ^1H and ^{13}C NMR, see Table S3, Supporting Information; HREIMS *m/z* 648.4039 $[M + Na]^+$ (calcd for $C_{41}H_{55}NO_4Na$, 648.4029).

3-*O*-[*N*-(Biphenyl)-*p*-carbamoyl]betulinic Acid (11): amorphous solid, $[\alpha]_D^{25}$+24.0 (*c* 0.30, $CHCl_3$); IR ν_{max} 3436, 3139, 2949, 2873, 1726, 1696, 1591, 1505, 1377, 1316, 1057, 973, 891, 839, 552 cm^{-1}; ^1H and ^{13}C NMR, see Tables 1 and 2; HREIMS *m/z* 674.4197 $[M + Na]^+$ (calcd for $C_{43}H_{57}NO_4Na$, 674.4185).

3-*O*-[*N*-(Allyl)carbamoyl]betulinic Acid (12): amorphous solid, $[\alpha]_D^{25}$ +19.4 (*c* 0.54, $CHCl_3$); IR ν_{max} 3454, 3151, 2949, 2873, 1699, 1505, 1455, 1376, 1275, 1136, 1106, 977, 891 cm^{-1}; ^1H and ^{13}C NMR, see Tables 1 and 2; HRESIMS *m/z* 562.3891 $[M + Na]^+$ (calcd for $C_{34}H_{53}NO_4Na$, 562.3872).

3-*β*-*O*-(Benzenesulfonyloxy)betulinic Acid (13): amorphous solid, $[\alpha]_D^{25}$ +15.4 (*c* 0.228, $CHCl_3$); IR ν_{max} 2979, 2949, 2870, 1698, 1798, 1731, 1642, 1450, 1359, 1175, 1098, 989, 939, 905, 591 cm^{-1}; ^1H and ^{13}C NMR, see Table S3, Supporting Information; HREIMS *m/z* 595.3453 $[M - H]^-$ (calcd for $C_{36}H_{51}O_5S$, 595.3457).

Acknowledgment. The Egyptian Government is acknowledged for the fellowship support to F.M.A.B.

Supporting Information Available: ^1H and ^{13}C NMR spectra of compounds **2**−**5** and **7**−**14**, full ^1H and ^{13}C NMR data assignments of **2**−**4**, **7**, **8**, **10**, and **13**, one dose (10.0 μM) mean graphs for **1** and **4** tested by DTP (Developmental Therapeutics Program) against the 60 human cell line panel, and the docked poses of compounds **5** and **12** in *S. cerevisiae* topoisomerase II DNA-binding domain. This material is available free of charge via the Internet at http://pubs.acs.org.

References and Notes

(1) Syrovets, T.; Bčhele, B.; Gedig, E.; Slupsky, R. J.; Simmet, T. *Mol. Pharm* **2000**, *58*, 71–81.
(2) Yun, Y.; Han, S.; Park, E.; Yim, D.; Lee, S.; Lee, C. K.; Cho, K.; Kim, K. *Arch. Pharm Res* **2003**, *26*, 1087–1095.
(3) Takasaki, M.; Konoshima, T.; Tokuda, H.; Masuda, K.; Arai, Y.; Shiojima, K.; Ageta, H. *Biol. Pharm. Bull.* **1999**, *22*, 606–610.
(4) (a) Yogeeswari, P.; Siram, D. *Curr. Med. Chem.* **2005**, *12*, 657–666. (b) Abdel Bar, F. M.; Zaghloul, A. M.; Bachawal, S. V.; Sylvester, P. W.; Ahmad, K. F.; El Sayed, K. A. *J. Nat. Prod.* **2008**, *71*, 1787–1790.
(5) Takada, Y.; Agrawal, B. B. *J. Immunol.* **2003**, *171*, 3278–3286.
(6) Fluda, S.; Scaffidi, C.; Susin, S. A.; Krammer, P. H.; Kroemer, G.; Peter, M. E.; Debatin, K. M. *J. Biol. Chem.* **1998**, *273*, 33942–33948.
(7) Tan, Y. M.; Yu, R.; Pezzuto, J. M. *Clin. Cancer Res.* **2003**, *9*, 2866–2875.
(8) Chowdhury, A. R.; Mandal, S.; Mittra, B.; Sharma, S.; Mukhopadhyay, S.; Majumder, H. K. *Med. Sci. Monit.* **2002**, *8*, BR254–265.
(9) Ganguly, A.; Das, B.; Roy, A.; Sen, N.; Dasgupta, S. B.; Mukhopadhayay, S.; Majumder, H. K. *Cancer Res.* **2007**, *67*, 11848–11858.
(10) Chowdhury, A. R.; Mandal, S.; Goswami, A. *Mol. Med.* **2003**, *9*, 26–36.
(11) Wang, J. C. *Annu. Rev. Biochem.* **1996**, *65*, 635–692.
(12) Champoux, J. J. *Annu. Rev. Biochem.* **2001**, *70*, 369–413.
(13) Deweese, J. E.; Osheroff, N. *Nucleic Acids Res.* **2009**, *37*, 738–748.
(14) Hsiang, Y. H.; Liu, L. F. *Cancer Res.* **1988**, *48*, 1722–1726.
(15) Jaxel, C.; Kohn, K. W.; Wani, M. C.; Wall, M. E.; Pommier, Y. *Cancer Res.* **1989**, *49*, 5077–5082.
(16) Staker, B. L.; Feese, M. D.; Cushman, M.; Pommier, Y.; Zembower, D.; Stewart, L.; Burgin, A. B. *J. Med. Chem.* **2005**, *48*, 2336–2345.
(17) Berger, J. M.; Gamblin, S. J.; Harrison, S. C.; Wang, J. C. *Nature* **1996**, *379*, 225–232.
(18) Stewart, L.; Redinbo, M. R.; Qiu, X.; Hol, W. G. J.; Champoux, J. J. *Science* **1998**, *279*, 1534–1540.
(19) Champoux, J. J. *J. Bio. Chem.* **1981**, *256*, 4805–4809.
(20) Wei, H.; Ruthenburg, A. J.; Bechis, S. K.; Verdine, G. L. *J. Biol. Chem.* **2005**, *280*, 37041–37047.
(21) Serge, C.-F.; Hugues-Olivier, B.; Anne, G.-L.; Arsene, D. G. P.; Olivier, M.; Remy, H.; Serge, F. *J. Med. Chem.* **2004**, *47*, 6840–6853.
(22) Vystrcil, A.; Pouzar, V.; Keřček, V. *Collect. Czech. Chem. Commun.* **1973**, *38*, 3902–3911.
(23) Macías, F. A.; Simonet, A. M.; Galindo, J. C. G.; Pacheco, P. C.; Sánchez, J. A. *Phytochemistry* **1998**, *49*, 709–717.
(24) Manabe, S.; Sugioka, T.; Ito, Y. *Tetrahedron Lett.* **2007**, *48*, 787–789.
(25) Burns, D.; Reynolds, F. W.; Buchanan, G.; Reese, B. P.; Enriquez, G. R. *Magn. Reson. Chem.* **2000**, *38*, 488–493.
(26) Shinkre, B. A.; Raisch, K. P.; Fan, L.; Velu, S. E. *Bioorg. Med. Chem. Lett.* **2007**, *17*, 2890–2893.
(27) Fluda, S.; Friesen, C.; Los, M.; Scaffidi, C.; Mier, W.; Benedict, M.; Nunez, G.; Krammer, P. H.; Peter, M. E.; Debatin, K. M. *Cancer Res.* **1997**, *57*, 4956–4964.
(28) Ballini, R.; Marcantoni, E.; Torregiani, E. *J. Nat. Prod.* **1997**, *60*, 505–509.
(29) Jesberger, M.; Davis, T. P.; Barner, L. *Synthesis* **2003**, *13*, 1929–1958.
(30) Kim, D. S. H. L.; Pezzuto, J. M.; Pisha, E. *Bioorg. Med. Chem. Lett.* **1998**, *8*, 1707–1712.
(31) El Sayed, K. A.; Laphookhieo, S.; Yousaf, M.; Prestridge, J. A.; Shirode, A. B.; Wali, V. B.; Sylvester, P. W. *J. Nat. Prod.* **2008**, *71*, 117–122.
(32) Sarek, J.; Klinot, J.; Dzubak, P.; Klinotova, E.; Noskova, V.; Krecek, V.; Korinkova, G.; Thomson, J. O.; Janostakova, A.; Wang, S.; Parsons, S.; Fischer, P. M. *J. Med. Chem.* **2003**, *46*, 5402–5415.
(33) *SYBYL* Molecular Modeling Software, version 8.0; Tripos Associates: St. Louis, MO, 2007; http://www.tripos.com.
(34) Clark, M.; Cramer, R. D., III; van Opdenbosch, N. *Comput. Chem.* **1989**, *10*, 982–1012.
(35) Stewart, J. J. *J. Comput. Aided Mol. Des.* **1990**, *4*, 1–105.
(36) Kellenberger, E.; Rodrigo, J.; Muller, P.; Rognan, D. *Proteins* **2004**, *57*, 225–242.
(37) Jain, A. N. *J. Med. Chem.* **2003**, *46*, 499–511.
(38) Welch, W.; Ruppert, J.; Jain, A. N. *Chem. Biol.* **1996**, *3*, 449–462.
(39) Ruppert, J.; Welch, W.; Jain, A. N. *Protein Sci.* **1997**, *6*, 524–533.

NP900312U